Dissipative vector solitons in a dispersion-managed cavity fiber laser with net positive cavity dispersion

H. Zhang[1], D. Y. Tang[1],*, L. M. Zhao[1], X.Wu[1] and H.Y.Tam[2]

[1] *School of Electrical and Electronic Engineering, Nanyang Technological University, Singapore, 639798*
[2] *Department of Electrical Engineering, Hong Kong Polytechnic University, Hong Kong, China*
*Corresponding author: edytang@ntu.edu.sg

Abstract: We report on the experimental observation of dissipative vector solitons (DVSs) in a dispersion-managed cavity fiber laser with large net positive cavity group velocity dispersion (GVD). Both the frequency-locked and phase-locked DVSs were observed. In addition, formation of multiple DVSs and DVS harmonic mode-locking were also experimentally revealed. Numerical simulations are in agreement of the experimental observations on the DVS formation in the fiber lasers.

References and links

1. L. M. Zhao, D. Y. Tang, and J. Wu, "Gain-guided soliton in a positive group dispersion fiber laser," Opt. Lett. **31**, 1788-1790 (2006).
2. L. M. Zhao, D. Y. Tang, T. H. Cheng, and C. Lu, "Gain-guided solitons in dispersion-managed fiber lasers with large net cavity dispersion," Opt. Lett. **31**, 2957-2959 (2006).
3. P. A. Bélanger, "Stable operation of mode-locked fiber lasers:similariton regime," Opt. Express **15**, 11033-11040 (2007).
4. O. G. Okhotnikov, T. Jouhti, J. Konttinen, S. Karirnne, and M. Pessa, "1.5-µm monolithic GaInNAs semiconductor saturable-absorber mode locking of an erbium fiber laser," Opt. Lett. **28,** 364-366 (2003).
5. M. Jiang, G. Sucha, M. E. Fermann, J. Jimenez, D. Harter, M. Dagenais, S. Fox, and Y. Hu, "Nonlinearly limited saturable-absorber mode-locking of an erbium fiber laser," Opt. Lett. **24,** 1074-1076 (1999).
6. N. Akhmediev , A. Buryak, and J. M. Soto-Crespo, "Elliptically polarized solitons in birefringent optical fibers," Opt. Commun. **112**, 278-282 (1994).
7. S. T. Cundiff, B. C. Collings, N. N. Akhmediev, J. M. Soto-Crespo, K. Bergman, and W. H. Knox, "Observation of Polarization-Locked Vector Solitons in an Optical Fiber, " Phys. Rev. Lett. **82**, 3988-3991 (1999).
8. H. Zhang, D. Y. Tang, L. M. Zhao, and H. Y. Tam, "Induced solitons formed by cross polarization coupling in a birefringent cavity fiber laser," Opt. Lett. **33**, 2317-2319 (2008).
9. D. Y. Tang, L. M. Zhao, B. Zhao, and A. Q. Liu, "Mechanism of multisoliton formation and soliton energy quantization in passively mode-locked fiber lasers," Phys. Rev. A **72**, 043816 (2005).
10. N. N. Akhmediev, A. Ankiewicz, M. J. Lederer, and B. Luther-Davies, "Ultrashort pulses generated by mode-locked lasers with either a slow or a fast saturable-absorber response," Opt. Lett. **23**, 280-282 (1998).
11. H. Zhang, D. Y. Tang, L. M. Zhao, and N. Xiang, "Coherent energy exchange between components of a vector soliton in fiber lasers," Opt. Express **16**, 12618-12623 (2008).
12. J. Wu, D. Y. Tang, L. M. Zhao, and C. C. Chan, "Soliton polarization dynamics in fiber lasers passively mode-locked by the nonlinear polarization rotation technique," Phys. Rev. E **74**, 046605 (2006).

1. Introduction

Recently, formation of dissipative solitons in pure normal-dispersion-cavity fiber lasers passively mode locked by the nonlinear polarization rotation (NPR) technique was reported [1-2]. It was shown that formation of the solitons is a result of the mutual nonlinear interaction among the normal cavity dispersion, cavity fiber nonlinear Kerr effect, laser gain saturation and gain bandwidth filtering. Although the NPR mode-locking process of the lasers unavoidably affected the detailed soliton features, it was found that its effect on the soliton shaping was minor [3]. In addition, both the experimental and theoretical studies have shown

that the dissipative solitons formed in the large net positive cavity GVD regime have very different characteristics from those formed in the net negative cavity GVD fiber lasers, and the differences can be traced back to the different soliton shaping mechanisms in the two cavity dispersion regimes. Mode-locking of a fiber laser can also be achieved with other techniques, e.g. using a semiconductor saturable absorption mirror (SESAM) [4, 5]. Different from the NPR mode locking, mode-locking with a SESAM requires no polarizer in the laser cavity, which potentially allows the formation of a DVS in the laser cavity.

Formation of both the frequency locked and phase locked DVSs in the negative GVD regime were theoretically predicted by Akhmediev et al. [6], and experimentally observed in a fiber laser mode-locked with a SESAM [7]. Different from a dissipative soliton formed in the negative GVD regime, a dissipative soliton formed in the large positive GVD regime has different soliton shaping mechanism, and furthermore is strongly frequency chirped. It would be interesting to find out whether a phase-locked DVS could be formed in a fiber laser with large net positive cavity dispersion or not. In this letter we will address this question. We show experimentally that either the polarization rotating or the phase-locked DVSs can be formed in the fiber lasers. In addition, we also show that multiple vector solitons with identical soliton parameters and harmonic mode locking of the vector solitons can be formed in the fiber lasers. Numerical simulations are found in agreement of the experimental observations, which confirm the DVS formation in the fiber lasers.

2. Experimental setup

Our experimental setup is shown in Fig. 1. The fiber laser has a ring cavity consisting of a piece of 1.5 m, 2880 ppm Erbium-doped fiber (EDF) with a GVD of about 40.8 ps^2/km, a total length of 3.5 m standard single mode fiber (SMF) with GVD of about -23 ps^2/km and 18.2 m dispersion compensation fiber (DCF) with GVD of about 2.55 ps^2/km. The total cavity length is 23.2m. Mode-locking of the laser is achieved with a SESAM. A polarization independent circulator was used to force the unidirectional operation of the ring and simultaneously incorporate the SESAM in the cavity. Note that within one cavity round-trip the pulse propagates twice in the SMF between the circulator and the SESAM. The laser was pumped by a high power Fiber Raman Laser source (BWC-FL-1480-1) of wavelength 1480 nm. A 10% fiber coupler was used to output the signals. The SESAM used is made based on GaInNAs quantum wells. It has a saturable absorption modulation depth of 5%, a saturation fluence of 90 µJ/cm^2 and a recovery time of 10 ps. The central absorption wavelength of the SESAM is at 1550nm.
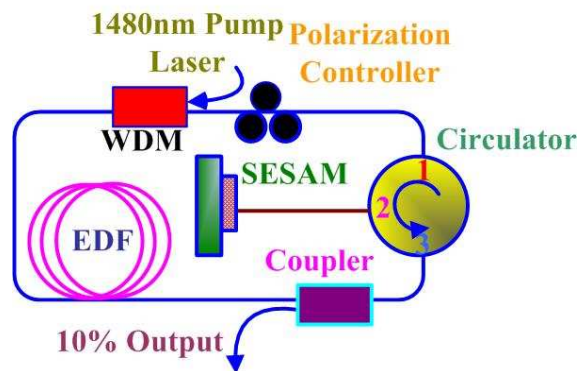

Fig. 1. Schematic of the fiber laser. SESAM: semiconductor saturable absorber mirror; PC: polarization controller; WDM: wavelength-division multiplexer; EDF: erbium-doped fiber.

3. Experimental results

This fiber laser has a typical dispersion-managed cavity with net normal cavity GVD of about 0.027ps^2. To control the net cavity GVD, DCF with different lengths were inserted between

the circulator and the SESAM. When the net cavity GVD was anomalous, it was observed that the spectrum of the mode-locked pulses had the typical features of those of the DVS reported in [7]. Increasing the length of the DCF, the net cavity GVD shifted to large positive values, correspondingly, the soliton operation of the laser shifted to a new dissipative soliton regime. Experimentally, the self-started mode locking of the laser could still be easily achieved at a large positive cavity GVD.

Figure 2 shows a typical optical spectrum of the dissipative solitons of the laser obtained at a large net positive cavity GVD. The soliton spectrum has characteristic steep spectral edges. However, different from the dissipative solitons formed in the fiber lasers mode-locked with the NPR technique, the soliton consists of two orthogonal polarization components. To highlight the vector nature of the soliton, we let the soliton pulse train pass through a rotatable external cavity polarizer and compared the features of the pulse train before and after passing through the polarizer, either with a high speed oscilloscope or an RF-spectrum analyzer. We found that the soliton shown in Fig. 2(a) was a polarization rotating vector soliton. Polarization rotation of the soliton could be easily identified e.g. by the oscilloscope trace measurement. Without passing through the external polarizer, the soliton pulse had identical pulse intensity on the oscilloscope trace for each cavity roundtrip, while after passing through the polarizer it became varying with the cavity roundtrips as shown in Fig. 2(b). It indicates that the polarization of the soliton rotated along the cavity. Figure 2(a) also shows the autocorrelation trace of the vector soliton. It has a width (FWHM) of ~ 40ps. If a $sech^2$ pulse shape is assumed, the soliton pulse width is ~ 24ps. The 3dB spectrum bandwidth of the soliton is ~ 6.5 nm, which gives a time-bandwidth product about 18.9, indicating that the soliton is strongly chirped.
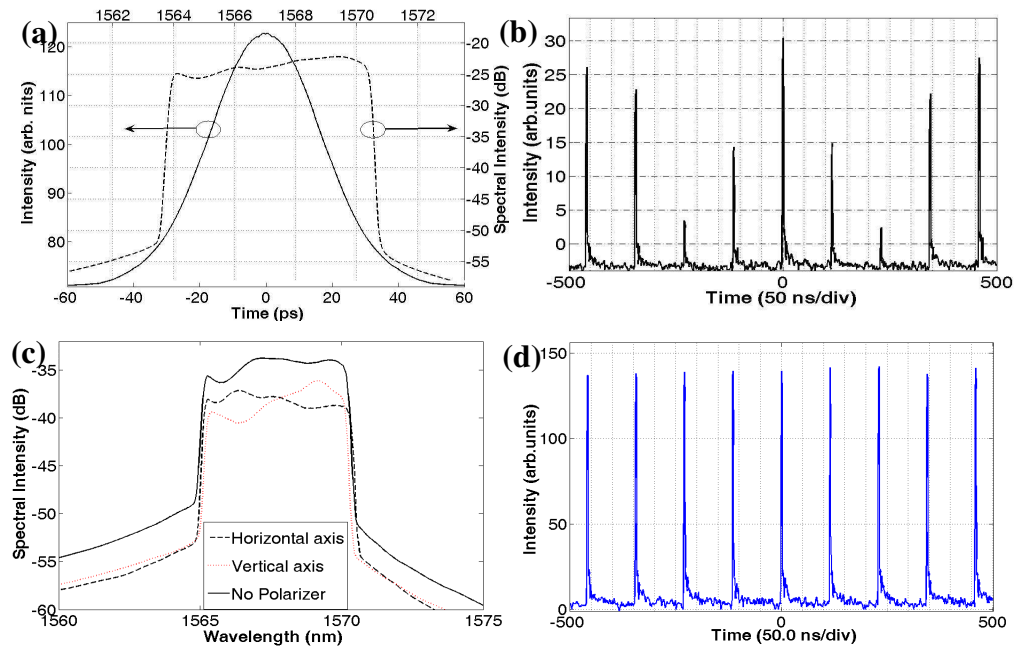

Fig. 2. (a) Spectrum and corresponding autocorrelation trace of a polarization rotating DVS emission state of the laser; (b) Oscilloscope trace of (a) after passing through a polarizer; (c) Polarization resolved optical spectra of a phase locked DVS emission state of the laser; (d) Oscilloscope trace of (c) after passing through a polarizer.

Controlling the linear cavity birefringence through an intra-cavity polarization controller, polarization locked vector solitons were obtained. A polarization locked vector soliton has the

characteristic that it has a fixed polarization during circulation in the laser cavity. Correspondingly, after passing through an external cavity polarizer the pulse height of such vector solitons on the oscilloscope trace would have identical value as shown in Fig. 2 (d). For a phase locked vector soliton we could also measure its optical spectra along the long and the short polarization ellipse axes, as shown in Fig. 2(c). Different from the polarization resolved dissipative vector solitons formed in the net negative cavity GVD fiber lasers, no four-wave-mixing spectral sidebands could be identified. We believe their absence could be traced back to the large frequency chirp of the soliton. The two orthogonal polarization components shown in Fig. 2(c) have comparable spectral intensity and the same center wavelength, but clearly different spectral distributions. Experimentally, the phase locking between the two orthogonal polarizations was further confirmed by the polarization evolution frequency measurement as described in [7]. Apart from the above near circularly polarized polarization locked DVS, polarization locked DVSs with significant spectral intensity difference between the two orthogonal polarization components were also observed. In one case the spectral intensity difference at the center soliton wavelength was as large as 20 dB. We experimentally measured the peak power of the weak soliton component in the case. It was about 0.1W. With the pulse peak power it is impossible to form a soliton in the laser. Therefore, we believe it could be an induced soliton formed by the cross coupling with the strong soliton component [8].

Adjusting the polarization controller, the central wavelength of the DVSs could be altered in a wide range from 1560nm to 1575nm. However, as the central soliton wavelength is increased, the formed DVS becomes less stable. This could be due to that the central absorption wavelength of the SESAM is about 1550nm, which favors the formation of the DVS centered near 1550nm. Multiple DVSs with identical soliton parameters were also obtained under strong pumping. In this case, harmonic mode locking was frequently obtained. Fig. 3 illustrates a case where 8 DVSs were equally spaced in the cavity with a separation of about 14.5ns. Other harmonic mode locking states of the DVS were also obtained by simply varying the pumping strength.
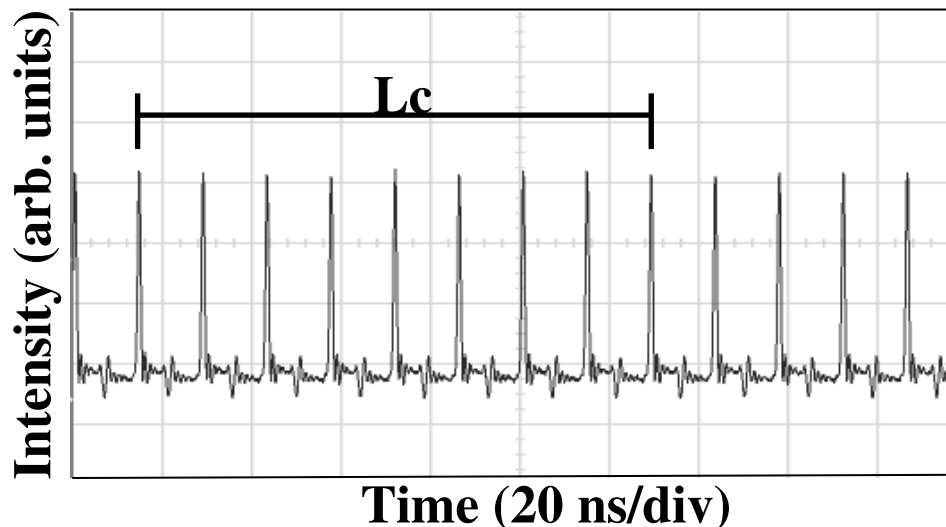

Fig. 3. Oscilloscope trace of a harmonically mode-locked gain-guided vector soliton state. Lc: cavity roundtrip time. 8 DVS coexist in cavity.

4. Numerical simulations

To gain an insight into the DVS formation, we also numerically simulated the operation of the laser. We used a round-trip model to include the laser cavity effects as well as the saturable

absorber effect in our simulations [9]. Briefly, we used the coupled Ginzburg-Landau equations to describe the pulse propagation in the weakly birefringent fibers:

$$
\begin{cases}
\dfrac{\partial u}{\partial z} = i\beta u - \delta \dfrac{\partial u}{\partial t} - \dfrac{ik^{''}}{2}\dfrac{\partial^2 u}{\partial t^2} + \dfrac{ik^{'''}}{6}\dfrac{\partial^3 u}{\partial t^3} + i\gamma(|u|^2 + \dfrac{2}{3}|v|^2)u + \dfrac{i\gamma}{3}v^2 u^* + \dfrac{g}{2}u + \dfrac{g}{2\Omega_g^2}\dfrac{\partial^2 u}{\partial t^2} \\[3mm]
\dfrac{\partial v}{\partial z} = -i\beta v + \delta \dfrac{\partial v}{\partial t} - \dfrac{ik^{''}}{2}\dfrac{\partial^2 v}{\partial t^2} + \dfrac{ik^{'''}}{6}\dfrac{\partial^3 v}{\partial t^3} + i\gamma(|v|^2 + \dfrac{2}{3}|u|^2)v + \dfrac{i\gamma}{3}u^2 v^* + \dfrac{g}{2}v + \dfrac{g}{2\Omega_g^2}\dfrac{\partial^2 v}{\partial t^2}
\end{cases}
$$

$$(1)$$

Where, u and v are the normalized envelopes of the optical pulses along the two orthogonal polarized modes of the optical fiber. $2\beta = 2\pi\Delta n/\lambda$ is the wave-number difference between the two modes and $L_b = \lambda/\Delta n$ is the beat length. $2\delta = 2\beta\lambda/2\pi c$ is the inverse group velocity difference. $k^{''}$ is the second order dispersion coefficient; k''' is the third order dispersion coefficient and γ represents the nonlinearity of the fiber. g is the saturable gain coefficient of the fiber and Ω_g is the bandwidth of the laser gain. For undoped fibers $g=0$; for erbium doped fiber, we considered its gain saturation as

$$
g = G\exp[-\frac{\int(|u|^2 + |v|^2)\mathrm{dt}}{P_{sat}}]
$$

$$(2)$$

Where G is the small signal gain coefficient and P_{sat} is the normalized saturation energy. The saturable absorption of the SESAM is described by the rate equation [10]:

$$
\frac{\partial l_s}{\partial t} = -\frac{l_s - l_0}{T_{rec}} - \frac{|u|^2 + |v|^2}{E_{sat}}l_s
$$

$$(3)$$

Where T_{rec} is the absorption recovery time, l_0 is the initial absorption of the absorber, and E_{sat} is the absorber saturation energy. To make the simulation possibly close to the experimental situation, we used the following parameters: $\gamma=3$ $W^{-1}km^{-1}$, Ω_g =16nm, P_{sat}=50 pJ, k''_{SMF}= -23 ps^2/km, k''_{EDF}=41 ps^2/km, k''_{DCF}=2.6 ps^2/km, k'''= -0.13 ps^3/km, E_{sat}=35 nJ, l_0=0.2, T_{rec}= 2 ps, and cavity length L= 23.2 m.

Numerically, it was found that under the current saturable absorber parameter selection, the formation of DVS in the laser is strongly the gain bandwidth dependent. When the gain bandwidth is large, i.e. 24nm, DVS is unable to form. In this case the spectrum of the mode-locked pulses has a Gaussian profile. Stable DVS is formed when the gain bandwidth is narrower than 16 nm. The narrower the gain bandwidth used for simulation, the smaller the spectrum bandwidth of the obtained DVS. Figure 4(a) shows a typical case of the calculated DVS evolution with the cavity roundtrips. Numerically we found that the total pulse intensity is unchanged with the cavity roundtrips, but intensity of the horizontal and the vertical component exhibits out-of-phase intensity variation, indicating that coherent energy exchange between them still exists [11]. After removing the four-wave-mixing terms from Eq. (1), such an out-of-phase intensity variation between the vector soliton components then disappeared. The calculated pulse width is about 20ps and its spectrum bandwidth is about 7 nm, which indicates that the formed DVS is strongly frequency chirped.

The result shown in Fig. 4 was obtained for a laser cavity with a beat length of L_b=100m. The DVSs formed have two orthogonal polarization components with comparable intensity and coincident central wavelength. Numerically, as L_b changed from 100m to 0.1m, i.e., increasing the cavity birefringence, intensity difference between the two orthogonal polarization components becomes larger, in accord with our experimental observations. We have also numerically investigated polarization evolutions of the formed DVSs by using the method reported in [12]. Depending on the cavity birefringence, either the polarization locked or polarization rotating DVSs were numerically obtained. Calculated based on the peak point of the DVSs, a polarization locked DVS has its polarization ellipse orientation fixed as it propagates along the cavity, while the polarization ellipse of a rotating DVS changes its

orientation along the cavity. The relative phase between the components of the polarization locked DVS at the pulse peak was always fixed at $\pi/2$. However, at the other points of the pulse it deviated from $\pi/2$, demonstrating the effect of frequency chirp. To determine how the frequency chirp of the solitons affects their polarization, we also numerically calculated the polarization states at different points of a pulse, e.g. at the pulse's peak and FWHM points. For the polarization locked DVSs it was found that the polarization ellipses calculated at different points had slightly different orientations, nevertheless, the difference remained the same along the propagation. This numerical result suggests that despite the strong frequency chirp of the DVSs, the temporal variation of their two orthogonally polarized components is always phase locked.
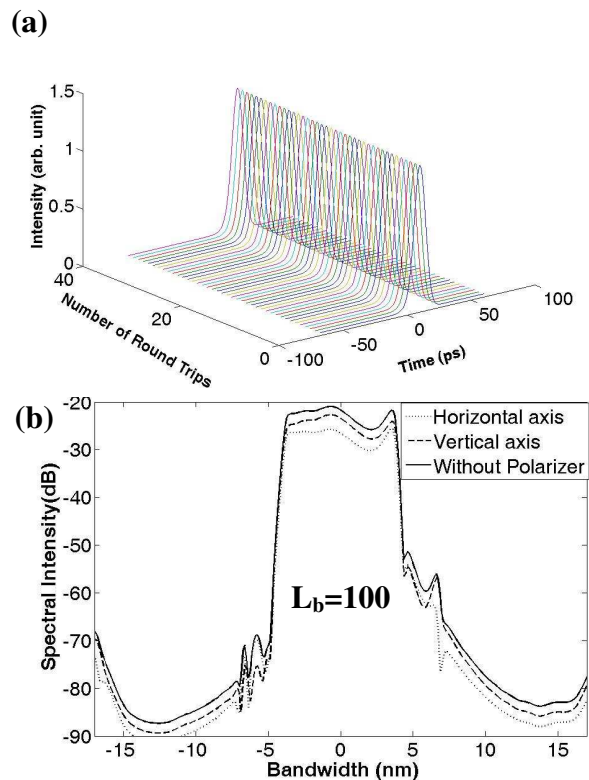

Fig. 4. (a) Combined pulse intensity evolution; (b) corresponding optical spectra numerically calculated.

5. Conclusion

In conclusion, DVSs have been experimentally demonstrated in a dispersion-managed fiber laser with large net normal cavity GVD. It was found that despite of the large frequency chirp of the dissipative solitons formed in the lasers, the polarization rotating and polarization locked DVSs could still be formed. In addition, formation of multiple DVSs with identical soliton parameters and stable harmonic DVS mode-locking are also experimentally obtained.

Acknowledgment